Original scientific paper *

NUMERICAL ASSESSMENT OF STRUCTURAL INTEGRITY AND FATIGUE LIFE OF AUTOMOTIVE LPG TANK AND MOUNTING COMPONENTS UNDER REGULATORY LOADING CONDITIONS

Miroslav Mijajlović[1], Miloš Milošević[1], Danijel Marković[1], Srđan Mladenović[1], Dušan Pribak[1]

[1]University of Niš, Faculty of Mechanical Engineering Niš, Serbia

Abstract. *A nonlinear finite element model was formulated to assess the structural integrity and fatigue life of an automotive LPG tank assembly comprising the cylindrical pressure vessel, clamping straps, holders, and telescopic supports. Experimentally characterized material properties and realistic frictional contacts were incorporated, while fluid–structure effects were approximated via mass–spring surrogates for sloshing and internal pressure. The assessment covered static and quasi-static scenarios (bolt pretensioning, tank filling) and dynamic conditions consistent with regulatory impacts of 8g lateral and 20g longitudinal accelerations. Vibrodynamic fatigue evaluation employed a Power Spectral Density methodology based on Welch's estimator to predict life under stochastic vehicle-induced excitation. Results indicate no catastrophic failure across loading regimes; however, mounting straps exhibit pronounced plasticity during tightening and accumulate ~91% fatigue damage at ten years, aligning with mandated replacement intervals. The pressure vessel shows negligible fatigue degradation and an unrealistically extended predicted life, motivating future work that incorporates cyclic filling/emptying through transient drive–idle–refuel sequences and derived load spectra. The methodology provides a rigorous computational basis for durability assessment and compliance verification of LPG tank installations while reducing reliance on extensive physical testing.*

Key words: *LPG tank structure, Finite Element Analysis, Structural integrity, Fatigue life prediction, Random vibration, Power Spectral Density*

1. INTRODUCTION

Safe mounting, fastening, and utilization of cylindrical LPG tanks in passenger and light commercial vehicles necessitate strict adherence to regulatory requirements and verification of structural integrity, either through experimental testing or numerical simulation. Previous studies addressing the integrity of automotive LPG systems have

emphasized the significance of structural performance following collision events, methodologies for leakage detection, and compliance with applicable regulations [1, 2].

The regulatory framework governing automotive LPG systems remains partially non-harmonized globally. Variations in the treatment of alternative fuel systems exist across regions, although the fundamental principles are consistent [3, 4]: (a) LPG tanks (cylindrical or toroidal) and associated equipment must be permanently installed within the vehicle; (b) design, material selection, manufacturing, installation, testing, marking, and periodic inspection procedures follow equivalent principles across jurisdictions; and (c) fuel quality must conform to standardized specifications.

UN/ECE Regulation No. 67 (R67) serves as the primary homologation standard for LPG equipment and vehicles in most EU countries and numerous signatories of the 1958 Agreement. The regulation comprises 2 sections: Part I – approval of specific equipment (tank, multivalve, safety devices, hoses, non-return valve, filter, ECU, housings, etc.); and Part II – installation requirements, including tank positioning and fixation (geometry, mechanical protection, prevention of gas intrusion into the cabin, ventilation), filling limited to 80% of nominal volume (via integrated limiter), safety valves (pressure relief devices and fusible plugs), and mandatory markings and documentation.

The Serbian Regulation on the Classification of Motor and Trailer Vehicles and Technical Requirements for Vehicles in Road Traffic [5] prescribes vehicle categories in accordance with international standards and defines technical requirements for construction, devices, and equipment, including safety elements, lighting and signaling systems, steering and braking devices, and alternative fuel installations such as LPG. It regulates homologation procedures, conformity certification, dimensional and mass limits, speed constraints, and mandatory auxiliary equipment, aiming to ensure traffic safety and harmonization with EN and ISO standards.

From the perspective of structural integrity and service life, R67 and national regulations stipulate: (1) tanks and components must be fully homologated; non-approved components are prohibited; (2) installation and fixation must comply with regulatory requirements; (3) maximum service life of LPG tanks is 10 years; (4) tanks may be filled to a maximum of 80% of volume; (5) tank-support connections must not induce structural damage (e.g., welding is prohibited); (6) washers under fastening bolts and nuts are mandatory; (7) bolts must meet at least strength class 8.8; (8) fuel containers must withstand accelerations without damage when full – 20g longitudinally and 8g laterally; and (9) validated numerical methods may be employed as an alternative to physical testing, subject to approval by the Technical Service.

2. RESEARCH OBJECTIVES

The primary objective of this research is to perform a numerical calculation of the mounting system for an LPG installation with telescopic pipes, with the aim of verifying compliance with prescribed operational requirements as well as assessing the structural integrity of the system.

The load-bearing capacity of LPG tank support structures has been investigated in detail, and several fundamental configurations exist. Jiang et al. [6] provide the basis for structural calculations of LPG systems. Doğru et al. [7] analyze the fatigue life and structural behavior of LPG tanks by combining experimental testing (material

characterization, hydrostatic tests, comparison of old and new tanks etc.) with numerical methods based on Finite Element Analysis (FEA). The main objective the work was the identification of critical stress zones, particularly in the lid area of the tank, and the extension of fatigue life through optimization of weld transition radii. J. Lv [8] examines the dynamic response of a vehicle-mounted tank using a rigid–flexible FEA model, demonstrating that the structure enters resonance regions at certain road frequencies. By optimizing the tank geometry, significantly lower stresses and higher natural frequencies are achieved, which improves vibration resistance and reduces structural mass.

3. DESCRIPTION OF THE STRUCTURE

The cylindrical automotive LPG tank (diameter D=300 mm, length L=650 mm, maximum volume V=42 l) is installed in the trunk of a family passenger vehicle (Fig. 1a).

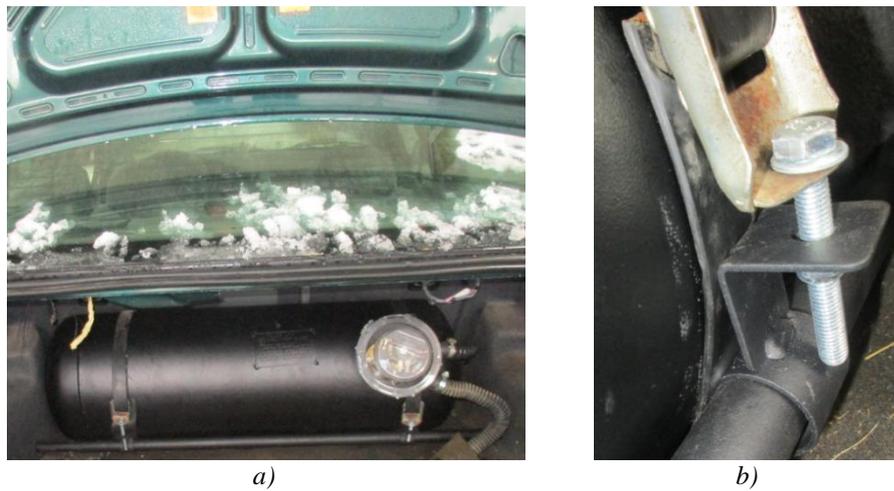*a)*   *b)*

Fig. 1 Cylindrical tank mounted on telescopic supports:a) complete structure, b) long bolt for tightening the belt around the tank via buckle and holder

Two parallel telescopic pipes (outer diameter 39.12 mm, inner diameter 34 mm, length 750 mm) are mounted to the side walls/chassis of the vehicles trunk. The pipes are not interconnected nor attached to the vehicle floor; they are fixed only to the side walls, i.e., directly to the chassis.

On the telescopic pipe, two holders per pipe are positioned to connect the tank with the pipes. The holders are fabricated from pipe segments (with larger diameter than the telescopic pipes) and L-profiles. The pipe segments and L-profiles are welded together, forming assemblies that can slide and rotate around the telescopic pipes. The holders are mounted so that the L-profiles face outward, one opposite to the other.

The tank is placed so that its lower surface rests on the telescopic pipes and holders. To avoid direct metal-to-metal contact, rubber pads are inserted at the contact points between the tank and the pipes/holders (Fig. 1b).

Permanent fixation and positioning of the tank is achieved using steel belts coated

with PVC/rubber (belt width 22 mm, length 1000 mm, steel thickness 0.7 mm, PVC/rubber thickness 2.4 mm). The belts, buckles, bolts, and nuts used for fastening the tank are shown in Fig. 2.

Fig. 2 Fastening components [9]

The metal belt is connected to the holder on the telescopic pipe closest to the rear seat of the vehicle by means of a short bolt (M8×20, strength class 8.8). At the opposite end of the belt, a buckle (length 50 mm, width 16 mm, thickness 1.5 mm) shaped as a curved letter "L" is attached. The belt is then passed over the tank and, through the buckle, connected to the holder on the other telescopic pipe using a long bolt (M8×50, strength class 8.8). By tightening the long bolt, the belt itself is tensioned. The belt is pressed firmly against the tank, securing it against the holders and telescopic pipes. The tank is fastened with two such belts.

4. MATERIALS AND MECHANICAL PROPERTIES

With the exception of the belts, which are a composite of steel and rubber, all other structural components are manufactured from steels (elastic modulus E=206 GPa).

Tank – P265NB (EN 10120): A pressure-vessel steel designed for cold-formed welded structures. It offers good toughness and weldability, with sufficient strength.

Belts – DX51D+Z (EN 10346) galvanized steel with rubber coating: A highly ductile, zinc-coated steel commonly used for flexible, corrosion-resistant applications. Its combination with rubber provides both elasticity and vibration damping.

Bolts and Nuts – 42CrMo4 (EN 10083): A high-strength alloy steel containing chromium and molybdenum. It exhibits excellent fatigue resistance, toughness, and wear resistance, making it suitable for critical fastening components.

Telescopic Pipes – P235TR1 (EN 10216-1): A non-alloy steel for pressure purposes, characterized by good mechanical properties and resistance to dynamic loading, suitable for structural pipes in automotive applications.

Washers and Buckles – C45 (EN 10083): A medium-carbon steel with balanced strength and toughness. It is widely used for mechanical parts requiring moderate wear resistance and dimensional stability.

Holders – S235JR (EN 10025): A structural steel with excellent weldability and adequate strength for load-bearing supports. It is commonly used in general construction and automotive frameworks.

The true stress-strain curves of the materials used are presented in Fig. 3. A multilinear isotropic hardening option is applied as an approximation of the actual material behavior up to the point of ultimate tensile strength.
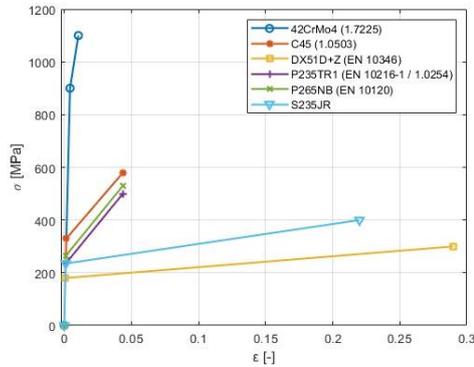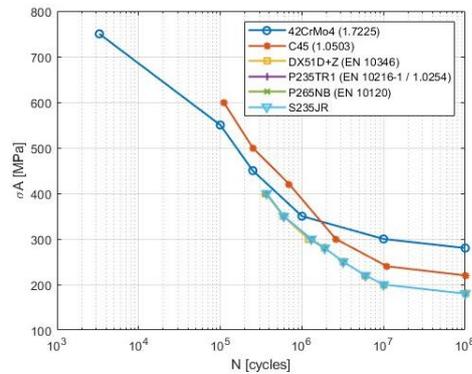

Fig. 3 True stress-strain curves for used materials [10]

Fig. 4 S-N curves for used materials [10]

The Wöhler (S-N) curves of the materials used are presented in Fig. 4. They are the basis for determining the service life and damage of the structure during operation.

5. LOADING OF THE TANK AND STRUCTURE

The entire assembly, consisting of the cylindrical LPG tank, belts, telescopic pipes, buckles, holders, bolts, washers, and nuts, is subjected to both static and dynamic loads.

The initial static loading is introduced through bolt pretensioning, which generates tensile forces in the clamping straps and induces stresses across all structural components. Subsequent filling of the tank with liquefied petroleum gas adds further static loading due to increased mass, while internal pressurization imposes circumferential and longitudinal stresses on the tank walls. Although filling and emptying are quasi-static processes that do not alter the primary loading mode, their cyclic nature over the service life must be considered in fatigue evaluation.

Dynamic loading of the tank and its structure arises from the dynamic behavior of the vehicle during motion and from the inertia of the tank, gas contained within, and the supporting components. The behavior of the vehicle in motion, and consequently of the tank and framing structure, is fully dynamic, cyclic, also stochastic.

6. FINITE ELEMENTS ANALYS

The numerical analysis (FEA) was performed using Ansys Workbench 19.2 Academic. As the first step, a CAD model was created, followed by appropriate

discretization of the model. Relevant initial and boundary conditions were applied, after which the model was loaded in accordance with the defined loading scenarios.

The numerical analysis comprised the following stages:

1. Modal analysis – conducted to verify model consistency, determine natural modes, and identify deformation shapes of the structure,

2. Quasi-static analysis of bolt tightening – the tank, as the primary component of the system, is secured solely by the tightening belts, which press the tank against the telescopic pipes and holders. Bolt tightening is performed up to a maximum of 50% of the material strength of the bolt shank (for the short bolt) and up to a maximum belt elongation of 2 mm due to tightening of the long bolt. Tightening is performed fast using a pneumatic gun.

3. Quasi-static analysis of tank filling with gas – after tightening, the tank is filled with LPG. The gas mass ($m_f \approx 20.2$ kg when the tank is filled to 80%) imposes additional static loading on the tank and supporting structure. When the tank is completely full, the gas pressure reaches 20 bar, further loading the tank walls.

4. Dynamic analysis (longitudinal) – the entire structure (tightened belts, full tank) was subjected to an acceleration of 20 g over 11 ms in the direction of vehicle motion (+y axis): acceleration from 0g to 20g in 5.5 ms, followed by deceleration back to 0g in the next 5.5 ms,

5. Dynamic analysis (transverse) – the entire structure (tightened belts, full tank) was subjected to an acceleration of 8 g over 11 ms in the direction perpendicular to vehicle motion (+x axis): acceleration from 0g to 8g in 5.5 ms, followed by deceleration back to 0 g in the next 5.5 ms,

6. Vibro-diagnostic analysis (RMS analysis) of the structure was performed to determine its service life (with the tank constantly full) under stochastic vibration conditions generated by the moving vehicle.

7. FINITE ELEMENT MODEL

The CAD model is employed as the foundation for the numerical analysis. The representation of the tank and the supporting structure for clamping and positioning is, in essence, equivalent to the actual three-dimensional construction, albeit with certain simplifications (Fig. 5).

In the CAD model, components with negligible influence on structural integrity were omitted. These include the identification plate of the tank, the rubber strips positioned between the tank and adjacent components to prevent metal-to-metal contact, as well as the welded seams connecting individual parts (tank–bottom and shell, supports–pipe and L-profile). The multivalve, the gas-tight housing surrounding the valve, and the multivalve holder were likewise excluded from the CAD model. However, their presence in the numerical analysis was represented by a mass point, assigned a mass equivalent to that of the neglected components. This mass point was positioned at the centroid of the multivalve, the most massive of the omitted elements. CAD models of bolts and nuts were adopted from the standard parts database, including threaded features.

Prior to discretization, the CAD model was refined: all bodies of complex topology were simplified by sectional cuts, resulting in a greater number of three-dimensional bodies within a single entity. The tank, telescopic pipes, and clamping straps, being

essentially thin-walled elements, were remodeled from the existing three-dimensional CAD model into two-dimensional representations in order to reduce computational demands [11]. All other bodies in the model remained three-dimensional (Fig. 6).
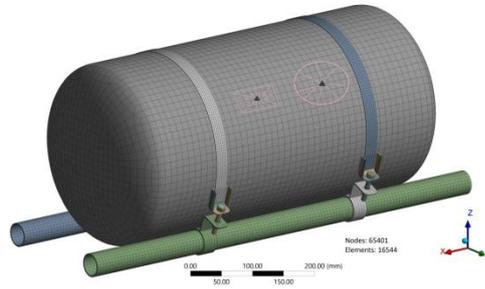

Fig. 5 CAD Model

Fig. 6 Discretized model

The interactions between bodies in the model were defined through frictional contacts, with friction coefficients assigned as follows: 0.12 for contacts representing threads, 0.3 for metal–metal contacts (telescopic pipes–supports), and up to 0.50 for contacts simulating metal–rubber–metal interfaces (strap–tank, supports–tank). These contacts were fully nonlinear but essential for achieving realistic analysis. Bolt–nut contacts were modeled as frictional only during the tightening phase; after tightening, they were converted into bonded contacts to prevent loosening of the nuts.

The multivalve, its holder, and housing were represented as a mass point of 0.8 kg, positioned at the centroid of the multivalve and connected to the corresponding tank nodes via an MPC element. The same principle is applied to the tank identification plate.
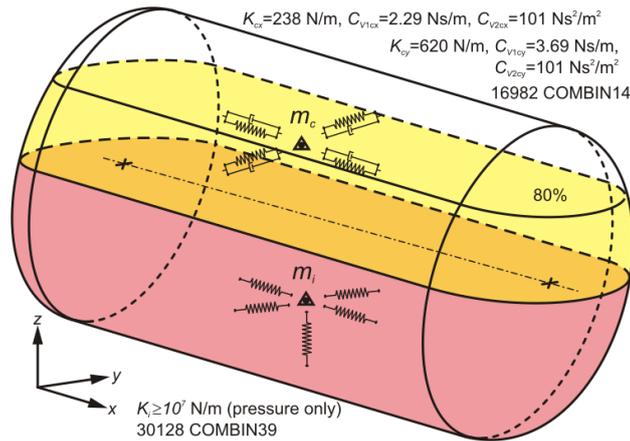

Fig. 7 Impulsive and convective mass in LPG tank

Modeling the fluid-tank interaction requires the application of a Fluid–Structure Interaction (FSI) model, which is highly demanding in terms of computational resources. For simplification, while maintaining physical realism, the LPG inside the tank was modeled as a mass point connected to the tank by springs. The Housner fluid model was adopted, in which the fluid mass is divided into an impulsive component (rigidly attached

to the tank, exerting wall pressure, $m_i \approx 0.7 \cdot m_f$) and a convective component (oscillating freely with a spring-like connection, causing sloshing, $m_c \approx 0.3 \cdot m_f$) [12, 13]. Accordingly, a mass point is defined at the centroid of each component (Fig. 7).

The impulsive mass, denoted as m_i, represents the portion of the fluid that does not exhibit sloshing motion and exerts pressure on the wetted areas of the tank walls due to its weight. The mass point m_i is connected to the tank nodes wetted by the impulsive mass (n_i) through nonlinear spring elements COMBIN39 [14]. These springs transmit only compressive forces to the tank. The total stiffness of these springs (K_i) is assumed to be sufficiently large to minimize the displacement of the mass point m_i, effectively constraining it to a value numerically close to zero. The stiffness of each individual spring is defined as the ratio of the total stiffness K_i to the number of springs n_i.

The convective mass is modeled as a mass point m_c located at the centroid of the volume it occupies in the static state and is connected to the walls by springs. The effect of the convective mass on the walls is dynamic in nature. The sloshing of the convective mass occurs predominantly in the longitudinal direction (y axis), although sloshing in the circumferential directions (x and z axes) is also present. To accurately model sloshing, elements COMBIN14 [15] are employed. These elements possess spring characteristics (K), linear damping (C_{V1}), and nonlinear damping (C_{V2}), shown in Fig. 7. Based on Housner's model and considering the sloshing direction (x and y), the appropriate spring coefficients are determined from the fundamental sloshing frequencies [13].

A constant load is defined as the gravitational acceleration acting in the negative -z axis direction. The only constraint imposed on the system is that the ends of the telescopic pipes are restricted from translating in all three directions, representing the physical connection of the telescope to the vehicle chassis.

8. MODAL ANALYSIS

The first 20 modes of the tank and the supporting structure are shown in Table 1.

Table 1 Structural Modes

Mode	Hz	Mode	Hz	Mode	Hz	Mode	Hz
1	61.031	6	366.26	11	748.44	16	1139.9
2	124.87	7	560.44	12	863.95	17	1171.1
3	131.41	8	587.72	13	949.17	18	1210.6
4	168.49	9	649.43	14	1018.4	19	1283.2
5	192.34	10	671.81	15	1087.2	20	1307.4

Figures 8 through 10 illustrate the total deformations of the entire structure for the 1st, 5th, and 6th modes. The first six modes are global modes that influence the overall structure; consequently, the frequency range most critical to the structural response spans from 61.031 Hz to 266.26 Hz. The remaining examined modes (from the 7th to the 20th, corresponding to 266.26 Hz to 1307.4 Hz) are of a local nature and are therefore of limited significance for further investigation.
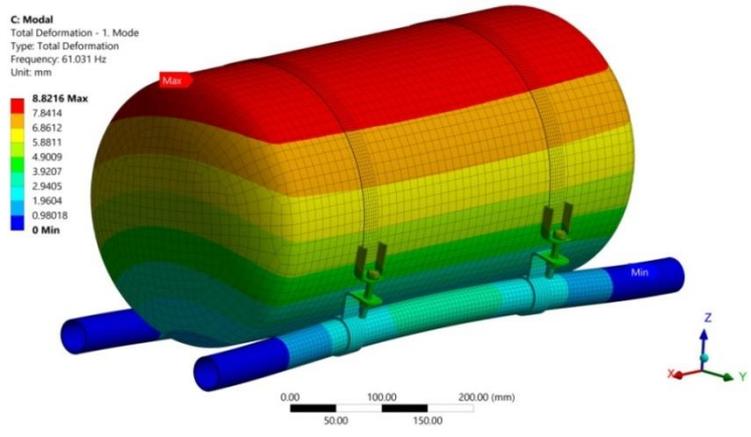
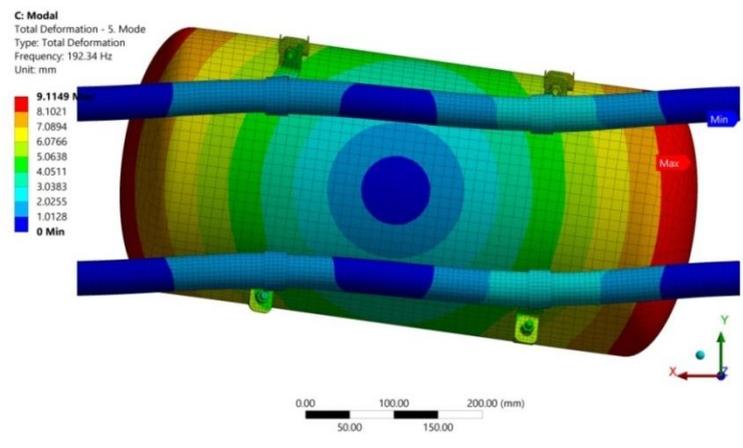**Fig. 8** Total deformation – Mode 1 (5:1)
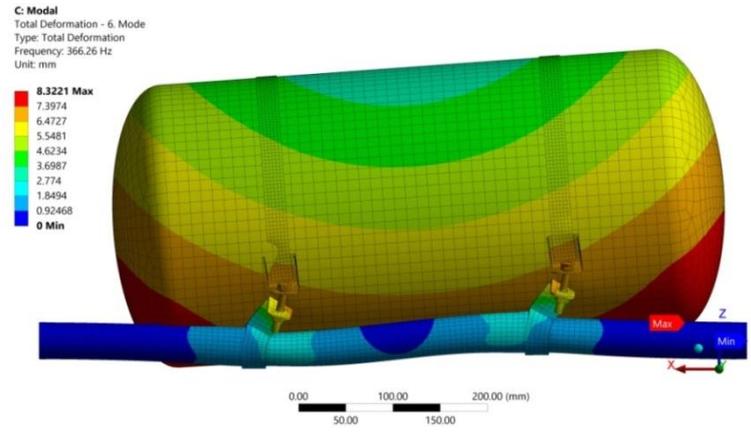

Fig. 9 Total deformation – Mode 5 (5:1)
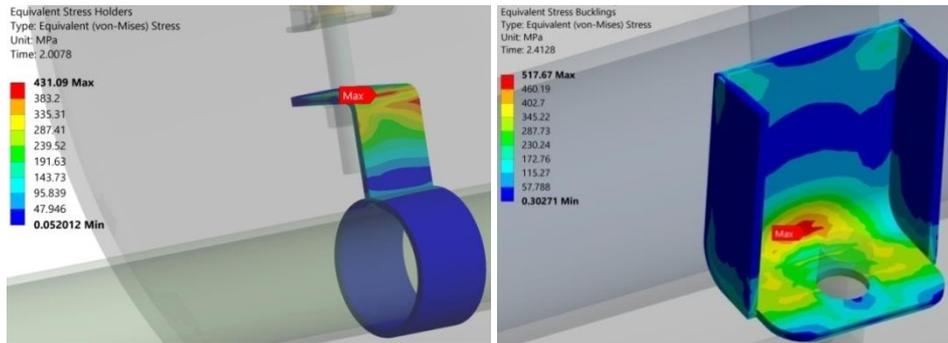

Fig. 10 Total deformation – Mode 6 (5:1)

Fig. 11 Max. Von Mises stress on the holders, bolt tightening (*t*=2.0078s)

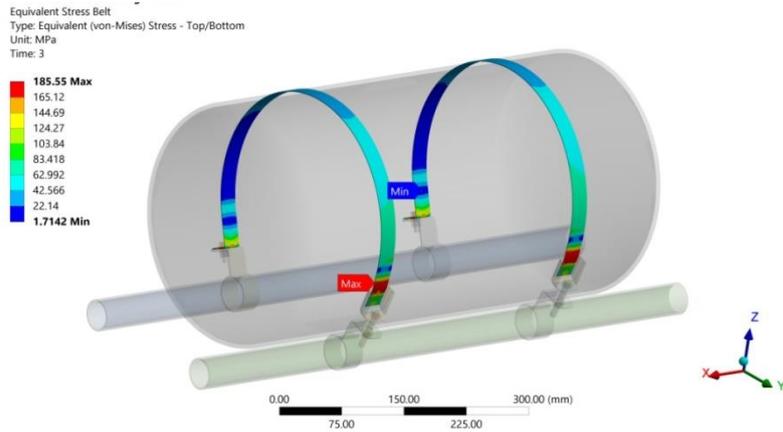**Fig. 12** Max. Von Mises stress on the buckling, bolt tightening (*t*=2.4128 s)

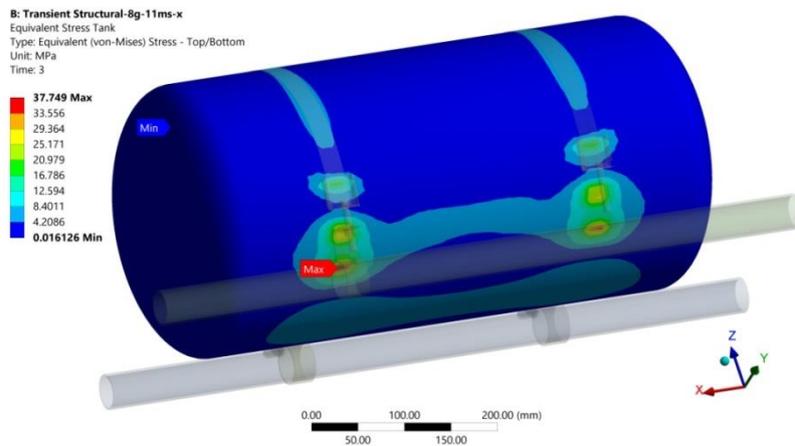**Fig. 13** Max. Von Mises stress on the straps during bolt tightening (*t*=3 s)

Fig. 14 Max. Von Mises stress on the tank during bolt tightening (*t*=3 s)

9. BOLT TIGHTENING

It is specified that all bolts shall be tightened simultaneously using a pneumatic torque gun. The long bolts apply tension to the straps, causing components to shift, deform, and become secured. During the tightening process, the holders located beneath the long bolts near bucklings are the first to move and undergo plastic deformation (Fig. 11-12).

The tensioning straps possess a substantial elastic reserve and therefore exhibit noticeable plastic deformation only at the final stage of the tightening process (Fig. 13).

During the tightening process, the tank undergoes only minor elastic deformations (Fig. 14), whereas the remaining components experience local contact-induced plastic deformations or remain within the elastic range.

10. TANK FILLING

The filling of the tank was simulated by applying an incrementally increasing mass at points m_i and m_c, which, through the connecting springs, load the lower half of the tank. The COMBIN14 elements remain inactive during this process, as no displacement of the mass points occurs. The increase in internal pressure within the tank was modeled as a pressure load, ranging from 0 bar, at the start of filling, to 20 bar at completion.

At the end of the filling process, the tank as a whole becomes more heavily loaded (Fig. 15), yet it remains within the elastic range.
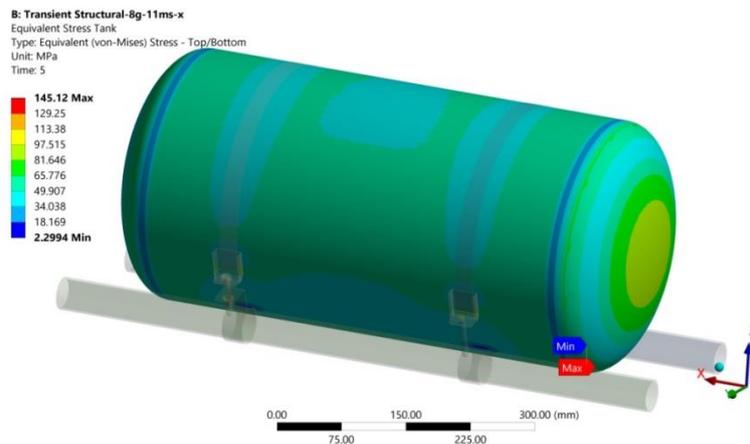

Fig. 15 Max. Von Mises stress on the tank during the filling process (t=5 s)

The "bulging" of the tank caused by the filling process further tightens the tensioning straps and increases the stress within them. The remaining components exhibit slight stress relief (see Figs. 16-18).
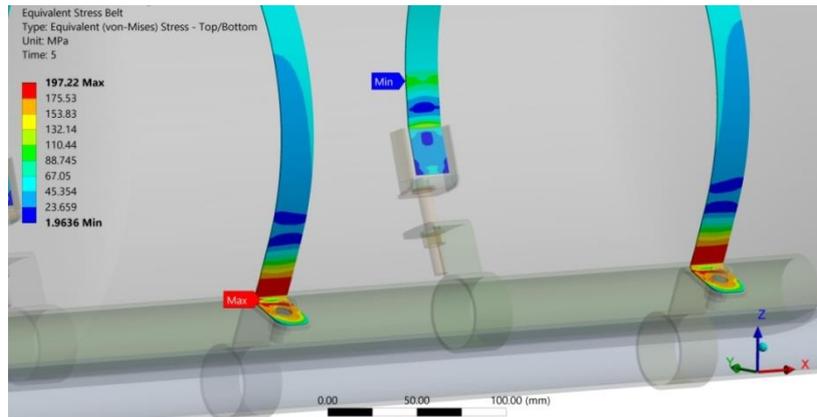
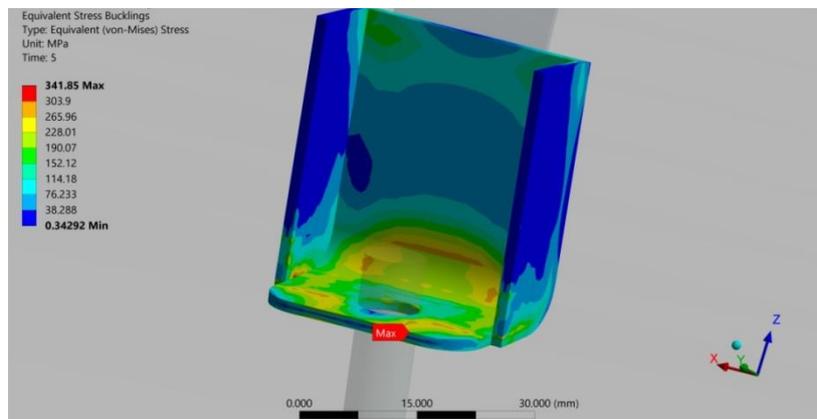**Fig. 16** Max. Von Mises stress in the straps during the filling process (*t*=5 s)

Fig. 17 Max. Von Mises stress in the bucklings during the filling process (*t*=5 s)
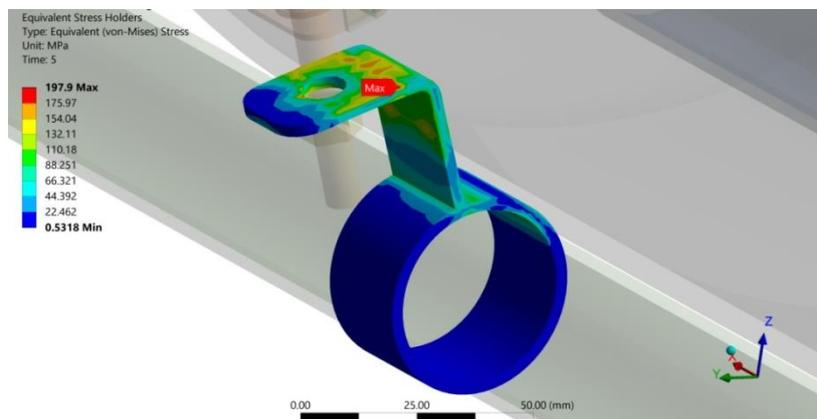

Fig. 18 Max. Von Mises stress in the supports during the filling process (*t*=5 s)

11. ACCELERATION OF 8G IN THE +X DIRECTION

Following the bolt-tightening and tank-filling processes, the structure was subjected to a shock load of 8g, applied for a duration of 11 ms in the +x direction. The stresses in all components increased by up to 9%, with only the straps (Fig. 20) and bucklings (Fig. 21) exhibiting stresses within the plastic range – yet remaining well below the ultimate strength and far from the failure zone. All other components remained within the elastic range. The stress distribution in the tank is shown in Fig. 19.
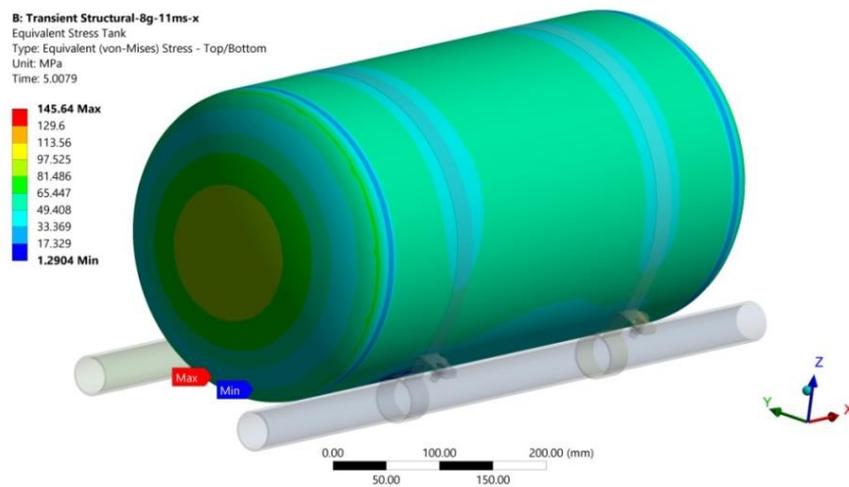

Fig. 19 Max. Von Mises stress in the tank during the 8g acceleration in the +x direction (t=5.0079 s)
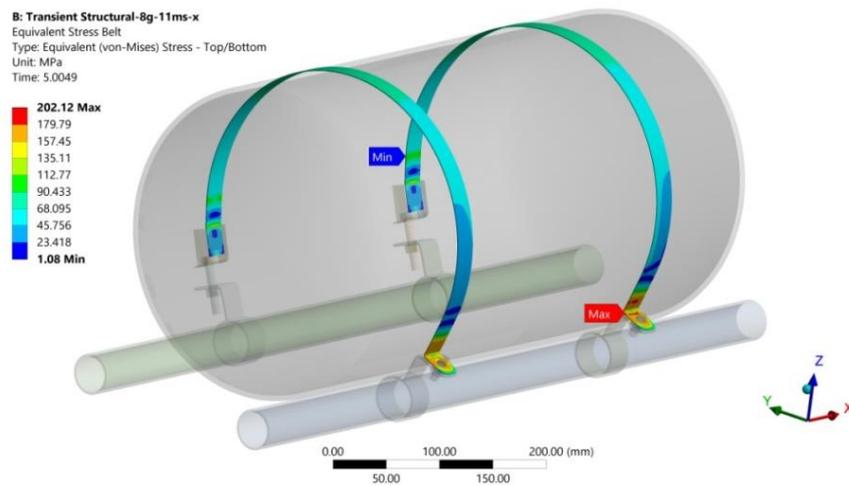

Fig. 20 Max. Von Mises stress in the straps during the 8g acceleration in the +x direction (t=5.0049 s)
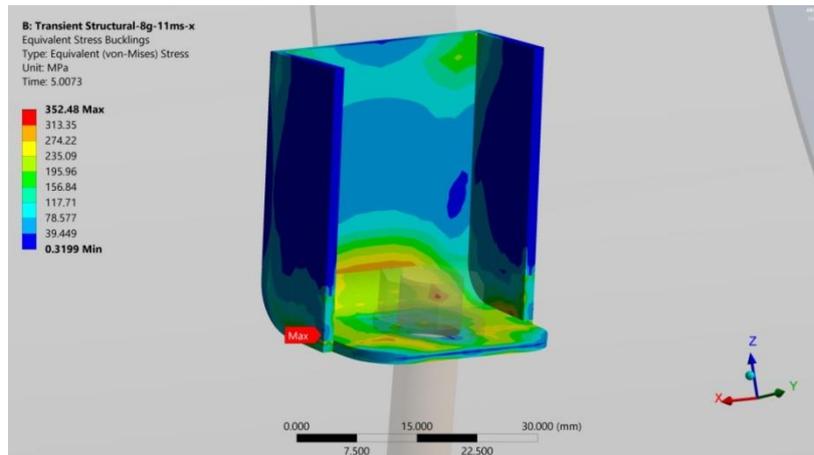
Fig. 21 Max. Von Mises stress in the bucklings during the 8g acceleration in the
+*x* direction (*t*=5.0073 s)

12. ACCELERATION OF 20G IN THE +Y DIRECTION

After the bolt-tightening and tank-filling processes, the structure was subjected to a shock load of 20g, applied for a duration of 11 ms in the +*y* direction. The stresses in all components increased by up to 18%, with only the tank, bolts, and nuts remaining within the elastic range. All other components exhibited stresses within the plastic range; however, these values were significantly below the ultimate strength and far from the failure zone. Figures 22 through 25 present the maximum stresses in the key components.
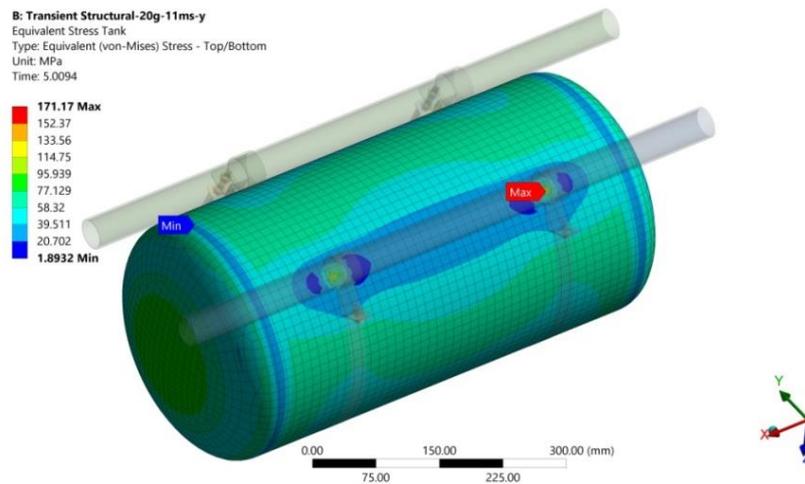

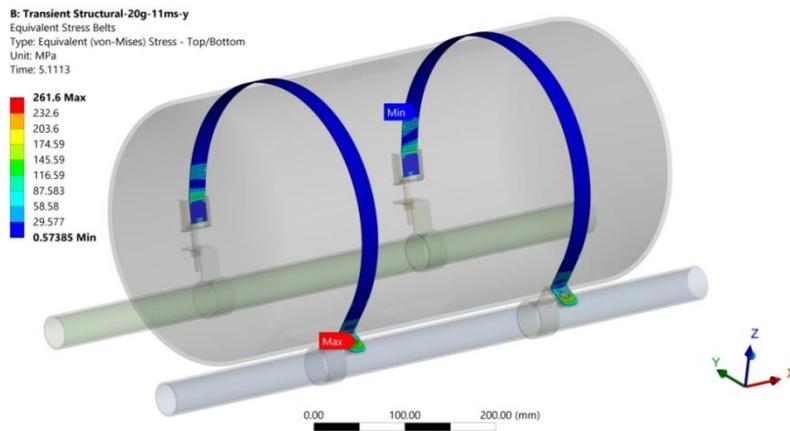**Fig. 22** Max. Von Mises stress in the tank, 20g in +*y* direction (*t*=5.0094 s)

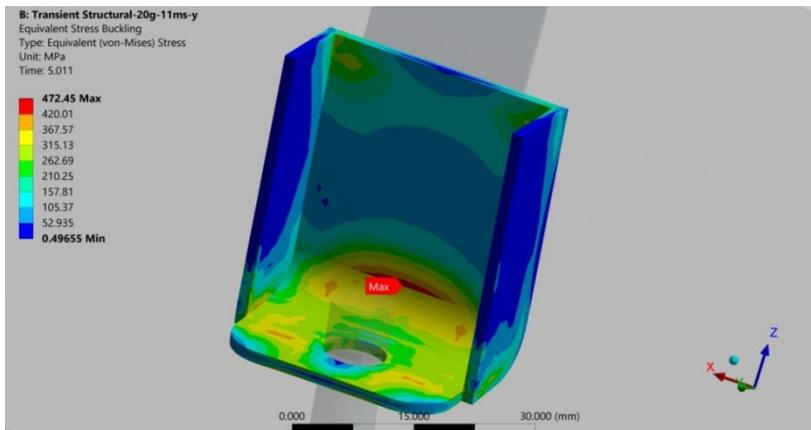**Fig. 23** Max. Von Mises stress in the straps, 20g in +*y* direction (*t*=5.1113 s)

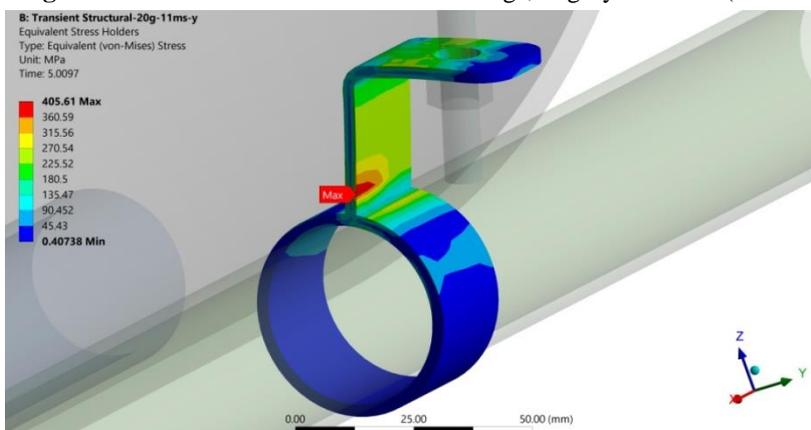**Fig. 24** Max. Von Mises stress in the bucklings, 20g +y direction (t=5.011 s)

Fig. 25 Max. Von Mises stress in the supports, 20g in +y direction (t=5.0097 s)

13. CONSOLIDATED VON MISES STRESS RESULTS FOR ALL COMPONENTS

For ease of analysis, Table 2 presents the stress values for all components under each of the enumerated structural loading conditions.

Table 2 Von Mises Stress [MPa] of all Components

	Bolt Pretension	Tank Filling	20 g/11 ms/y	8 g/11 ms/x
Tank (P265NB EN 10120)	37.749	145.12	171.17	145.64
Belt (DX51D+Z EN 10346)	185.55	197.22	261.60	202.12
Bucklings (C45/1.0503)	517.67	341.85	472.45	352.48
Holders (S235JR)	431.09	197.90	405.61	210.72
Pipes (P235TR1 EN 10216-1/1.0254)	256.32	185.25	304.91	218.26
Bolts (42CrMo4/1.7225)	814.33	417.35	833.61	455.36
Nuts (42CrMo4/1.7225)	538.49	309.78	567.75	319.47
Washers (C45/1.0503)	554.83	306.05	565.10	311.38

14. RANDOM VIBRATION LIFE AND DAMAGE

To perform damage analysis at a given moment or to predict the structural service life, it is essential to identify the sources of loading and potential damage. During the operation of the LPG tank and its fastening components, damage may result from bolt tightening, tank filling and emptying, fluid sloshing within the tank, and vibrations originating from the vehicle during motion. Previous analyses indicate that static or catastrophic failure of the tank and its components does not occur under normal operating conditions, although evidence of damage initiation has been observed.
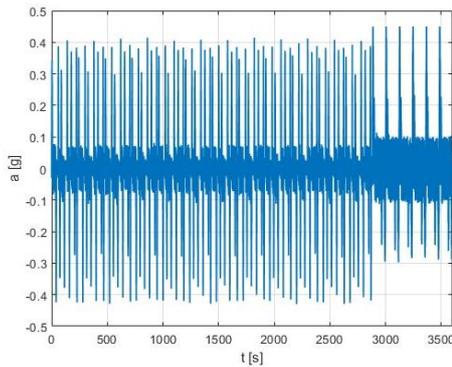

Fig. 26 Vehicle acceleration profile as a function of time
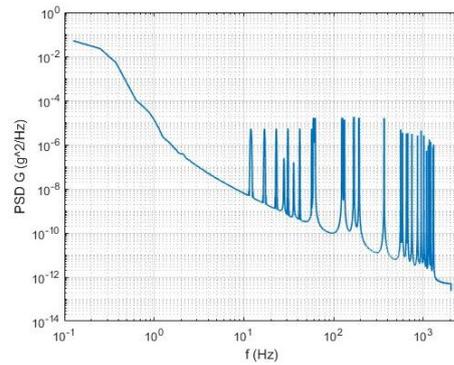
Fig. 27 Power spectral density (PSD) of tank acceleration expressed as a function of frequency

For the tank and its supporting structure, the primary source of vibration originates from the vehicle itself: engine vibrations, chassis vibrations, wheel-induced vibrations (due to road conditions), aerodynamic resistance, and others. Among these, wheel-induced vibrations associated with vehicle motion have the dominant influence. Statistically, a typical family car powered by LPG in Serbia travels approximately

15,000-20,000 km annually [16]. During driving, the acceleration-time profile generally exhibits mild to moderate speed variations, as the vehicle is primarily used in urban and suburban environments. In accordance with average road conditions and speed limits in Serbia, vehicle accelerations typically range within ±0.1 g during normal driving, with occasional peaks of 0.2g-0.5g during sudden acceleration or braking. For most of the time, acceleration remains relatively stable at constant speeds on open roads, whereas frequent oscillations occur in urban traffic due to stop-and-go driving. When this signal is analyzed in the frequency domain, very low frequencies (below 1 Hz) dominate, corresponding to slow speed changes, with occasional rapid spikes during gear shifts or obstacle avoidance [17]. Figure 26 illustrates the acceleration profile of a family vehicle as a function of time.

Based on the acceleration profile, the Power Spectral Density (PSD) for acceleration, denoted as PSD G, is generated using Welch's method. PSD G, expressed in units of g^2/Hz, indicates how the "power" of random acceleration is distributed across different frequency ranges of the structure [18].

Within the context of Random Vibration analysis, PSD G characterizes the statistically representative nature of the excitation applied to load the structure. Instead of using a realistically measured but time-consuming acceleration–time signal, only its spectral energy distribution across frequencies is defined, simplifying the computation.

Welch's method for PSD G estimation is based on segmenting the acceleration–time signal into multiple overlapping sections, applying a window function (e.g., Hann) to each segment, computing the FFT, and obtaining a periodogram for each segment. These periodograms are then combined to reduce the variance of the estimate. Subsequently, normalization by the frequency bandwidth is performed so that the result represents energy per unit frequency [19].

To ensure full coverage of the excitation energy range, it is recommended that the frequency span extend from 0 Hz (or from the 1st mode) up to a value exceeding 1.5 times the last significant mode (in this case, the 6th mode at 366.26 Hz). Figure 27 presents the calculated PSD G for a passenger vehicle equipped with an LPG system.
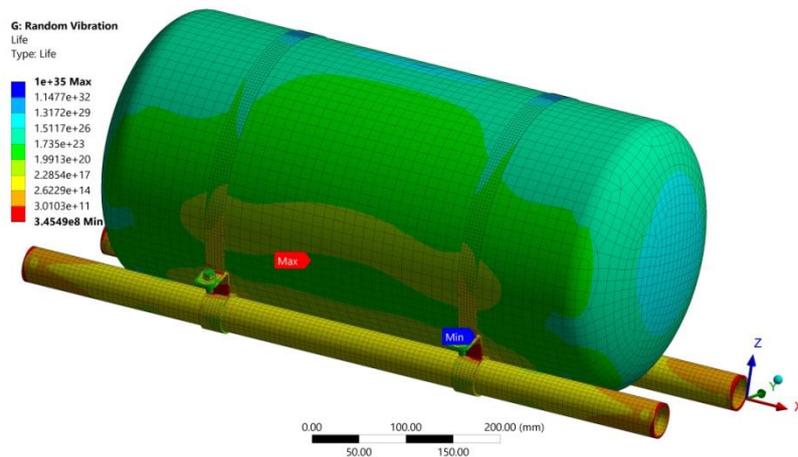

Fig. 28 Random Vibration Life

When the obtained PSD G is applied to the structure under clamping conditions, with the tank permanently filled with gas, the minimum service life is observed for the clamping strap closest to the multivalve and the gas-tight housing (Fig. 28). The computed service life of this strap is $3.4549 \cdot 10^8$ s ($\approx$10.95 years). Based on the proposed model the estimated service life of the tank is approximately 1,730,206 years.

When a service life of 10 years is assigned to the structure (corresponding to the maximum allowable operational life of the tank), an accumulated damage of 91.342% is obtained for the strap located closest to the multivalve (Fig. 29). This indicates that 91.342% of the component's fatigue life has been consumed.
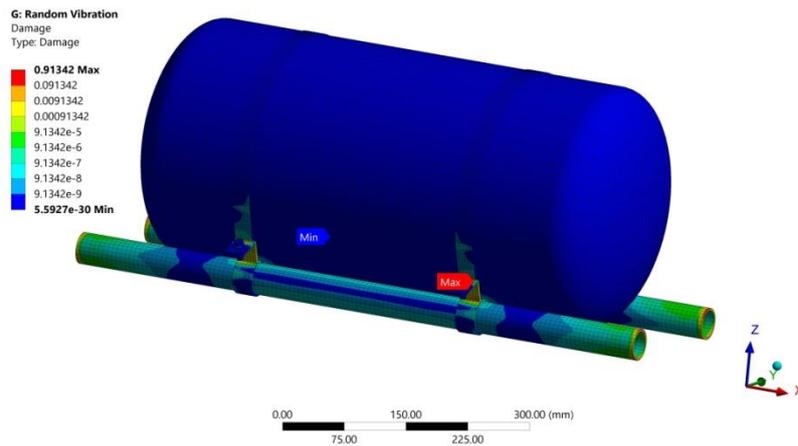

Fig. 29 Random Vibration Damage

The maximum damage observed on the tank is $5.5 \cdot 10^{-28}$%.

15. DISCUSSION AND CONCLUSIONS

A detailed numerical analysis was conducted on a cylindrical LPG tank mounted on telescopic pipes in the trunk of a family vehicle, with the objective of assessing the structural integrity throughout the legally prescribed maximum operational life of 10 years.

A complex numerical model was developed, accounting for the positioning and fastening of the tank, gas filling and its influence on the tank, internal fluid sloshing, exceptional events simulating frontal and lateral vehicle impacts, as well as fatigue assessment due to vehicle-induced vibrations. Materials used in the model correspond to those employed in actual components, with their relevant properties determined experimentally. The model incorporates realistic interactions between elements, including contact engagement/disengagement, frictional contacts, and stiffening effects. The model is fully nonlinear.

To optimize computational time, the two-sided fluid–structure interaction between the LPG gas-liquid phase and the tank was not explicitly modeled. Instead, it was

approximated using mass points attached to the tank walls via springs, simulating sloshing, gas pressure forces, and drag effects.

Fatigue assessment was performed under the assumption of stochastic vehicle vibrations. It was assumed that the vehicle covers an average mileage, operates under rational driving conditions, always within speed limits, and without exceptional events or any mechanical impact on the tank and its supporting structure. The tank was considered fully filled (80% of its maximum volume) and maintained at maximum pressure (20 bar) throughout the fatigue assessment. The influence of relatively rapid filling and slow emptying during operation on tank fatigue was not considered in the analysis.

The analysis of tank positioning and fastening (tightening of long bolts to secure the straps and press the tank against its supports and telescopic pipes) revealed that nearly all components-except the tank, nuts, and bolts-undergo plastic deformation during the tightening process. The greatest plastic deformation occurs in the straps, followed by the holders and bucklings. None of the components are at risk of static failure; however, damage to components is evident.

Tank filling introduces additional loading on the tank, straps, and bucklings due to tank expansion and increased mass. Supports, nuts, bolts, washers, and pipes are partially relieved as the telescopic pipes slightly separate, redistributing the load among all components. The tank remains within its elastic limit, and plastically deformed components are not endangered by static failure.

Lateral loading of the structure with an acceleration of 8g over 11 ms does not significantly stress the tank-the fluid inside rises during the "impact," which alleviates structural loading. The inertia load is primarily absorbed by the straps, bucklings, bolts, and, to a lesser extent, the supports and telescopic pipes. No static failure occurs, although some components enter the plastic zone. Fluid stabilization within the tank imposes additional loading on the straps, resulting in their maximum stress occurring after the acceleration ceases.

Longitudinal loading of the structure with an acceleration of 20g over 11 ms tilts the tank in the direction of acceleration; however, the tank itself does not experience stress sufficient to cause static failure. The most heavily loaded components are the bucklings, bolts, straps, supports, and pipes. All components, except the tank, enter the plastic zone and sustain significant damage, yet static failure does not occur.

Summarizing the loading results, it is concluded that catastrophic structural failure does not occur under static, quasi-static, or dynamic loading conditions.

Vibrodynamic analysis for fatigue assessment indicates that the most stressed components (straps, bucklings, supports) fail first. The strap closest to the multivalve fails first, after approximately 11 years of operation. This result aligns with regulatory requirements stipulating that most LPG system components should be replaced after 10 years of service. The analysis shows that the strap accumulates approximately 90% damage after 10 years of operation.

The vibrodynamic analysis of the tank indicates an unrealistically long service life and an extremely low level of damage after 10 years of use. These results would be significantly more realistic if cyclic filling and emptying of the tank were considered. However, PSD-based analysis cannot account for filling/emptying as a vibrational influence (since the vehicle remains stationary during filling, and vibrations occur regardless of whether the tank is full or empty). A realistic fatigue analysis of the tank would require a transient simulation of driving with emptying, stationary periods, filling,

followed by load spectrum generation and extrapolation for 10 years. This could represent a future direction of analysis if necessary. Neglecting filling and emptying does not compromise the validity of results for other components.

REFERENCES

1. Packard, M. H, Stoltzfus, D, 2017, *Evaluation of Methodology for LPG Fuel System Integrity Tank Test*, NHTSA Technical Report, Washington, USA.
2. Lynch, L. A et al, 2021, *Evaluation of Safety Standards for Fuel System and Fuel Container Integrity of Alternative Fuel Vehicles*, NREL/TP-5400-77455, Denver, USA.
3. United Nations Economic Commission for Europe (UNECE). Regulation No. 67 – Uniform provisions concerning the approval of specific equipment of motor vehicles using liquefied petroleum gases (LPG). EUR-Lex – Official Journal of the European Union. 2008; L72:1-112.
4. United Nations Economic Commission for Europe (UNECE). Regulation No. 115 – Uniform provisions concerning the approval of: I. specific LPG (liquefied petroleum gases) retrofit systems to be installed in motor vehicles for the use of LPG in their propulsion system, Official Journal of the European Union. 2014; L323:91-137.
5. Republic of Serbia: Rulebook on the Classification of Motor and Trailer Vehicles and on the Technical Requirements for Vehicles in Road Traffic, Official Gazette of the Republic of Serbia. 2012;40/2012 (amended: 102/2012, …, 110/2022 – other rulebook, 48/2023, 24/2024, 101/2024, 53/2025).
6. Jiang M et al, *Analysis of key points in strength design of LPG storage tank support structure*, Proc SPIE MEMAT 2023;13082:130821K.
7. Doğru, M. H., & Göv, İ., Experimental Verification of the LPG Tank Material and Improvement of the Fatigue Life According to Lid Geometry by using FEA Technique, MECHANIKA, 2019.
8. J. Lv, Analysis of dynamic response characteristics of vehicle-mounted tank based on the finite element method, Journal of Vibroengineering, Vol. 28, No. 1, –16, 2025,
9. https://www.lpgcngturkey.com/?page_id=1486 (last access: 11.01.2026).
10. Colás, R, Totten, G. E, 2016, Encyclopedia of Iron, Steel, and Their Alloys (5-volume set). CRC Press. ISBN 1466511044.
11. Milić P, Marinković D, Ćojbašić Ž, 2023. CAD-based FE modeling of thin-walled structures. Innovative Mechanical Engineering;2(1):52–63
12. Li Y-C, Gou H-L. 2018, *Modeling Problem of Equivalent Mechanical Models of a Sloshing Fluid*. Shock and Vibration.
13. Jaiswal R, Kulkarni S, Pathak P, 2008. Study on sloshing frequencies of fluid-tank system. 14th World Conference on Earthquake Engineering (14WCEE).
14. https://www.mm.bme.hu/~gyebro/files/ans_help_v182/ans_elem/Hlp_E_COMBIN39.html (last access: 11.01.2026).
15. https://www.mm.bme.hu/~gyebro/files/ans_help_v182/ans_elem/Hlp_E_COMBIN14.html (last access: 11.01.2026).
16. CarVertical: Newsletter 2025, https://www.carvertical.com/rs (last access: 28.12.2025).
17. Lopes R, et al, 2023, *A dynamic response analysis of vehicle suspension system*. Appl Sci.
18. Lee S, 2025, Mastering Welch's Method in Signal Processing: A Comprehensive Guide to Power Spectral Density Estimation. NumberAnalytics.
19. Sharma S, Chouksey M, Pare V, Jain P, 2020, Modal and frequency response characteristics of vehicle suspension system using full car model. IOP Conf Ser Mater Sci Eng. 2020.